RSC Advances

ROYAL SOCIETY OF CHEMISTRY

www.rsc.org/advances

Cite this: DOI: 10.1039/c0xx00000x

www.rsc.org/xxxxxx

ARTICLE TYPE

Actuation Based on Thermo/Photosalient Effect: Biogenic Smart Hybrid Driven by Light and Heat

Subash Chandra Sahoo,[a] Naba K. Nath,[a] Lidong Zhang,[a] Mohamad H. Semreen,[b] Taleb H. Al–Tel,[b] Panče Naumov[a]*

Received (in XXX, XXX) Xth XXXXXXXXX 20XX, Accepted Xth XXXXXXXXX 20XX
DOI: 10.1039/b000000x

Aimed at the design of efficient smart actuating materials, we have fabricated a self–actuating material that sets the platform for conceptually new, hybrid biocompatible actuators capable of dual mechanical response—by changes in temperature and by stimulation with weak ultraviolet or blue visible light. We demonstrate herein that microcrystallites of thermosalient and photosalient (leaping) solids can effectively utilize thermal or light energy and act as a robust and dynamically active "skeleton" to actuate sodium caseinate films as an elastic, flexible, biocompatible, natural protein matrix, similar to artificial muscle. The spectroscopic, kinematic and mechanical profiles of the new material are all consistent with a mechanism whereby the cooperative strains induced by reshaping and motions of the thermosalient crystals trigger macroscopic mechanical deformation of the matrix. The elastic medium absorbs the stress, thus providing a reinforcing feedback to the brittle crystals. The hybrid material conveniently combines fast energy absorption and conversion within single crystals and elasticity of polymers and displays a remarkable improvement in the tensile properties relative to the non–doped caseinate. Being based on natural protein, this thermally and photoresponsive artificial muscle is also biologically compatible and environmentally benign.

Introduction

The currently available artificial actuating materials are based on thermo/photoactive elastomers[1–8] supplemented by active photo/thermo switching chemical groups that are either dispersed throughout the polymer matrix as solid solutions or are chemically coupled to the polymer backbone as appendages to or crosslinks between the polymer strands. In either case, externally induced activation of the individual switching units of the dopant molecules that are isolated by the polymer host triggers spatial rearrangements in the polymer chains. In effect, collective perturbations at macroscopic scale appear as deformation (bending or curling) of the doped elastomeric beams and shells. Depending on the dopant, normally a single chemical type of switching response can only be elicited by a single stimulus (light or temperature); for instance, the most commonly utilized azobenzene unit, capable of *trans–cis* isomerization, is responsive to excitation by light.[9–15] While similar materials have proven convenient mechanistic models and have contributed greatly to better understanding of the actuation with elastomeric beams, their performance is inherently limited by the weak coupling between the incident light or thermal energy and the mechanical energy, unfavourable directionality vectors, and low order parameters.[16–22] Taken together, these shortcomings result in poor kinetics with slow operation and extended recovery times. Moreover, being normally fabricated out of synthetic polymers, the dynamic elements based on such hybrid elastomers or liquid crystals[23–28] would require extensive chemical modification to attain the biocompatibility requirements for artificial biological elements such as tissues and muscles. These impediments necessitate a conceptually new approach to the design of thermo/photomechanical actuators.

There is an increasing body of evidence that under mechanically applied force certain molecular crystals can respond with impressive elastic properties, which could be utilized for rapid, reversible and fatigueless (photo) mechanical actuation to mimic the motility of natural systems. Indeed, there are now a number of reported examples of organic and metal-organic molecular crystals which respond to external impact with impressive elastic moduli.[29–32] Although they normally experience stronger force for the same displacement and undergo small absolute deformations, extraordinarily large local photoresponsive stresses can be anticipated for the dense and ordered packing of such single crystals. As an additional advantage relative to the photostrictive inorganic ceramics[33] that is currently utilized to control actuators, crystal engineering approaches[34–36] can be readily utilized with molecular crystalline materials to generate multicomponent variants (salts, mixed crystals, cocrystals or solvates) to quantify the statistical dilution effects or modulate their mechanical performance profile.

Whilst aiming at fabrication of a new class of biocompatible, compostable, nontoxic actuating materials that mimic natural actuating tissues, we have embarked on exploration microcrystallites of **thermosalient solids**, a class of extremely

rare self–actuating crystalline materials.[37–38] When heated or cooled close to the thermosalient solid–solid phase transition—occasionally associated with martensitic–type transitions—these unique materials respond to the supplied heat by building up a colossal internal strain. On passing over the transition, the strain that has developed inside the crystal is suddenly released. In response to the change of the supramolecular environment, rapid molecular rearrangement occurs triggering a visually astonishing mechanical response—crystals perform jumps whereby they propel themselves to travel over distances 10^4–10^5 their own size in less than a millisecond!

Herein, we describe a potentially very useful application of this effect to prepare a unique, mechanically robust, "all−in−one" biomimetic hybrid platform based on a combination of thermosalient crystals and a natural polymer that responds mechanically to both light and temperature. To secure preservation of macroscopic integrity of single crystals, we match the superior actuating capabilities of such thermosalient crystalline "skeleton" to an elastic and mechanically reinforcing scaffold casted out from a natural and entirely compostable natural protein matrix as "tissue". The resulting flexible and mechanically robust hybrid biomimetic artificial muscle conveniently combines the remarkable actuating capability of the thermosalient single crystals with the biocompatibility of the natural polymer; it can be fabricated with controllable composition and thickness, and has superior mechanical profile relative to the non–doped polymer. During the characterization we accidently discovered that in addition to heating, the new material also mechanically responds reversibly to ultraviolet light. The dense and ordered structure of the crystalline component provides a platform for faster energy transfer with low energy dissipation and enhanced coupling between the light and mechanical energy. Such composite, multi–responsive actuator presents a conceptually new approach to the design of actuating materials and is a direct mimic of some natural mechanically responsive elements.

Results and discussion

Preparation of the films

As a mechanically responsive, actuating component we selected thermosalient crystals of phenylazophenyl palladiumhexafluroacetylacetonate (PHA).[39] If heated over the phase transition around 90 °C, crystals of the yellow–orange phase (α) of PHA transform to the dark red high–temperature phase (β); if they are unfixed to the surface, the crystals undergo sudden and forceful jumps to land at distances that vary from several millimetres to several centimetres from their original position.[39]

To prepare mechanically robust, elastic smart hybrids with controllable composition and thickness, by in situ crystallization we embedded crystals of this thermosalient material into a mechanically reinforcing scaffold casted out of sodium caseinate (NaCas) as a biogenic protein matrix. Swollen, hot aqueous mixtures of NaCas were mixed with PHA solution in presence of a plasticizer, casted into polystyrene or PTFE molds with controllable depth, and stabilized in controlled humidity during 1–3 days (See Figure S1, in the Supporting Information, (SI) for details on the synthetic procedures). The originally turbid mixtures afforded clear, elastic orange thin films (Figures 1B and C). While pure NaCas films prepared under identical conditions without the dopant were colorless, soft and gelatinous, the doped films were orange, elastic and notably tougher. They also had a cellophane-like appearance. Unlike NaCas, the doped films are also very elastic and when folded bend easily without cracking. When the pressure is removed, they quickly revert back to their original shape. If pulled at both ends, strips of the doped films do not tear easily (see the results of the mechanical characterization below). SEM images of the surface of the films show a large amount of crystals ca. 1–4 μm and a small amount of thin needle crystals >15 μm in length embedded in the film, some of which are protruding out of the film surface. The phase identity of these crystals with the polymorph α of pure PHA was conformed from the UV–visible spectra (see below). Upon strong heating, the films steadily loose water up to 160 °C with the maximal weight loss occurring due to dehydration at 105 °C (Figures S7 and S8, SI).

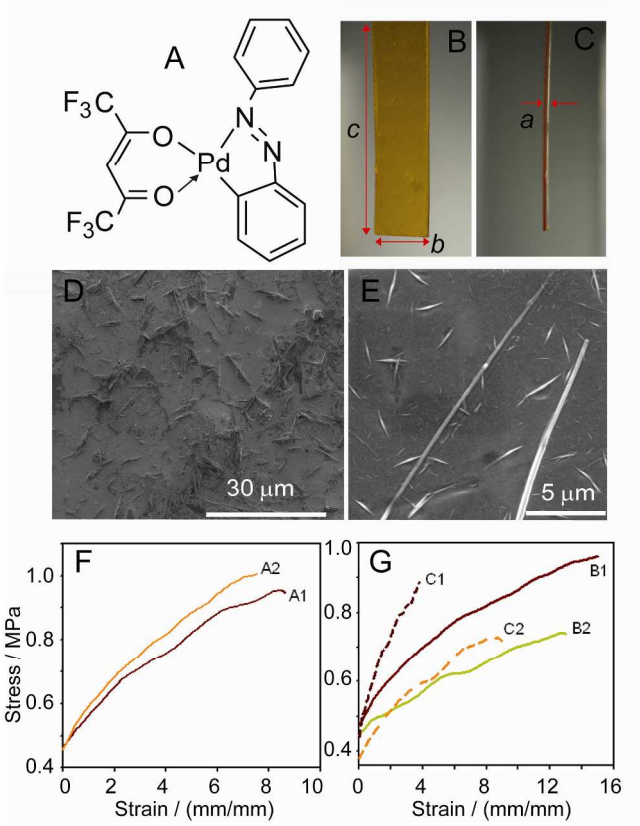

Fig. 1 Morphology and surface structure of sodium caseinate (NaCas) films doped with phenylazophenyl palladiumhexafluroa-cetylacetonate (PHA; A). (B, C) Optical micrographs of a strip ($a \times b \times c$ = 0.02 × 2 × 11 mm) cut out from a larger PHA–doped thin film. (D, E) SEM images of the film surface showing the acicular crystals of PHA embedded in the protein matrix. (F, G) Effects of the dopant concentration and film thickness on the tensile proper-ties of the films. The content of PHA in samples A1 and A2 was 0.1 and 0.2% (w/w), respectively. The thickness of samples B1 and B2 (PHA–doped NaCas) and of samples C1 and C2 (non–doped NaCas) was 0.15 and 0.10 mm, respectively.

Mechanical characterization

To quantify the extent to which the new material can stretch and to assess its ability to withstand tensile forces, we performed

a series of comparative standard tensile tests on non-doped and doped films of various thickness and various concentrations of the dopant. As it can be inferred from Table S1 in the SI, NaCas films doped with PHA generally have larger Young's modulus and elongation relative to films from pure NaCas. The stress–strain profiles in Figure 1F indicate that the mechanical strength increases with increasing amount of the dopant, and that the elasticity and tenacity of the films can be effectively tuned by adjusting the PHA concentration. Higher dopant concentrations result in stronger and also stiffer films; change of the PHA content from 0.1 to 0.2% (w/w) appears as increase of the Young's modulus from 0.0557 to 0.0692 MPa. This mechanical reinforcement is accompanied by a 5.5–fold decrease in the maximum stretching, from 49.75% to 8.96%.

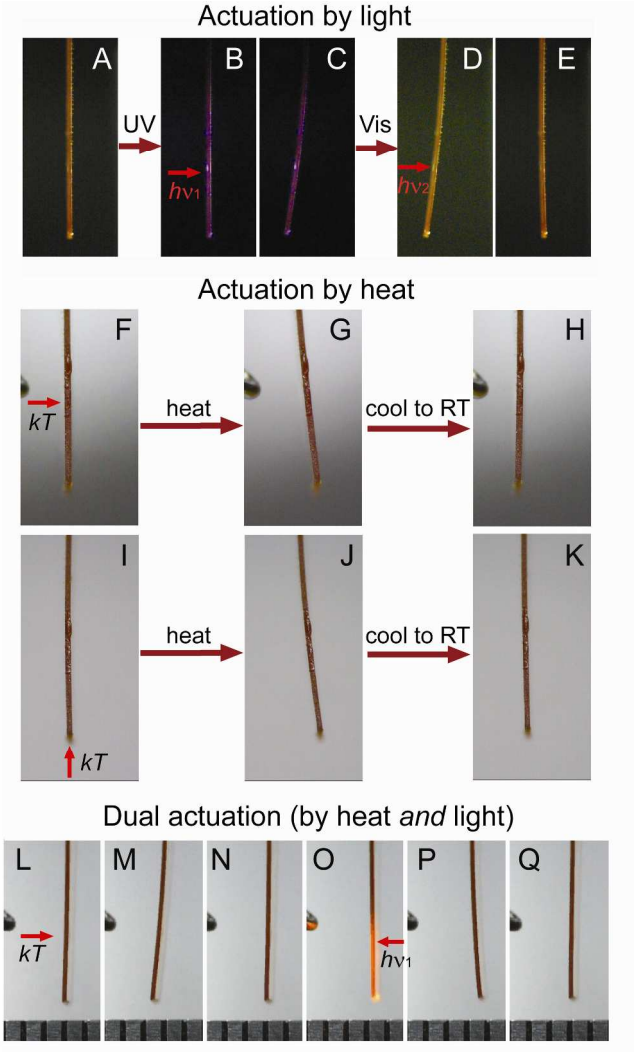

Fig. 2 Dual actuation of the PHA-doped sodium caseinate film shown in Fig. 1. Excitation at 375 nm (⊥*bc*; LEDs) of the film (A) induces visible bending (B, C). The bent film reverts to its original shape by exposure to white light (D, E). The same film (F, I) bends by lateral (∞*bc*, G), or axial (||*c*, J) heating, and reverts to its original shape after cooling (H, K). (L – Q) The film can be alternatively and repeatedly bent by exposure to heat (L – N) and light (O – Q).

To examine the effect of thickness of the films on their mechanical properties, we casted out samples from pure NaCas and PHA–doped NaCas in PTFE molds with variable thickness. As shown in Figure 1G and Table S1, thicker films of pure NaCas have smaller Young's modulus, but can be stretched more than thinner films. For pure (non–doped) NaCas film, the decrease of thickness from 0.15 mm to 0.10 mm reduces the Young's modulus from 0.1069 to 0.0386, while the maximum elongation increases from 21.15 to 47.65%. Doping with PHA crystals inverts the trend in ability to stretch; as shown in Figure 1G, reducing the thickness of the PHA-doped film from 0.15 mm to 0.10 mm decreases the Young's modulus from 0.0299 to 0.0220 MPa, and the maximum elongation from 87.15 to 72.15%. These results are in line with the overall hardening and reinforcing effect of PHA crystals on the film, which becomes particularly important at large cross-sections.

Actuating properties

As shown in Figures 2F–H, and it can also be inspected from the video recording deposited as Movie S1 in the SI, beams of PHA doped films of NaCas affixed at their top and hanging vertically bend visibly when approached laterally (⊥*bc*) with a pointy heating element or with a flat heating element from the bottom (axially, ||*c*) during 95 s (Figures 2I–K). The bending direction depends on the surface of the film exposed to the heat. For precise kinematic analysis, the deflection of the beam was tracked by mapping the trajectory of its tip extracted from the recorded videos (Figure S3, SI). For short heating times (during the first 10–15 seconds), the deflection depends linearly on the heating time (Figure 3A). This linear bending regime is followed by slower bending in response to the notable tensile strains that develop on both surfaces of the bent film and counter-balance the bending moment. The bending reaches a maximum after about 40 minutes from the onset of heating. The original shape of the film is recovered within 20–70 seconds after the heating source has been terminated. As shown in Fig S2 (SI), under identical conditions, non-doped NaCas films do not bend, in line with the assumption that the actuation is powered by the thermosalient effect of the PHA crystals. The DSC curves of pure yellow phase (α) PHA crystals (Figure S8, SI) have a saw-tooth appearance and evidence that the time profile of the thermosalient phase transition of PHA (α→γ) depends on the size of the crystals and occurs over a wide temperature range 69–83.5°C. The temperature of the phase transition could be even lower for smaller crystals, and these temperatures, at least locally, are reached during the heating of the films. A second, non–thermosalient and irreversible phase transition (γ→β) occurs 95.7°C. Correspondingly, strong heating of the hybrid films whereby embedded PHA crystals are transformed to the high–temperature β phase is detrimental to the mechanical response; it alleviates the actuating ability of the film, and results in thermal fatigue.

We also noticed that moderate, continuous and uniform axial heating from the bottom (||*c*) induces several auto-oscillations of the beam (Figure 3D; Movie S2 in the SI). This oscillating behaviour can be explained by a thermo-mechanical feedback, where the film bends to retract itself from the higher temperature. After the deflection, the tip of the film encounters a colder region of the temperature gradient. In response to the cooling, the film relaxes and straightens, thus re-entering the warmer region again. As it is heated, the beam deflects and the cycle is repeated. During 95 seconds of heating in our experiment, we observed three oscillations, each with duration of about 30 seconds (Figure

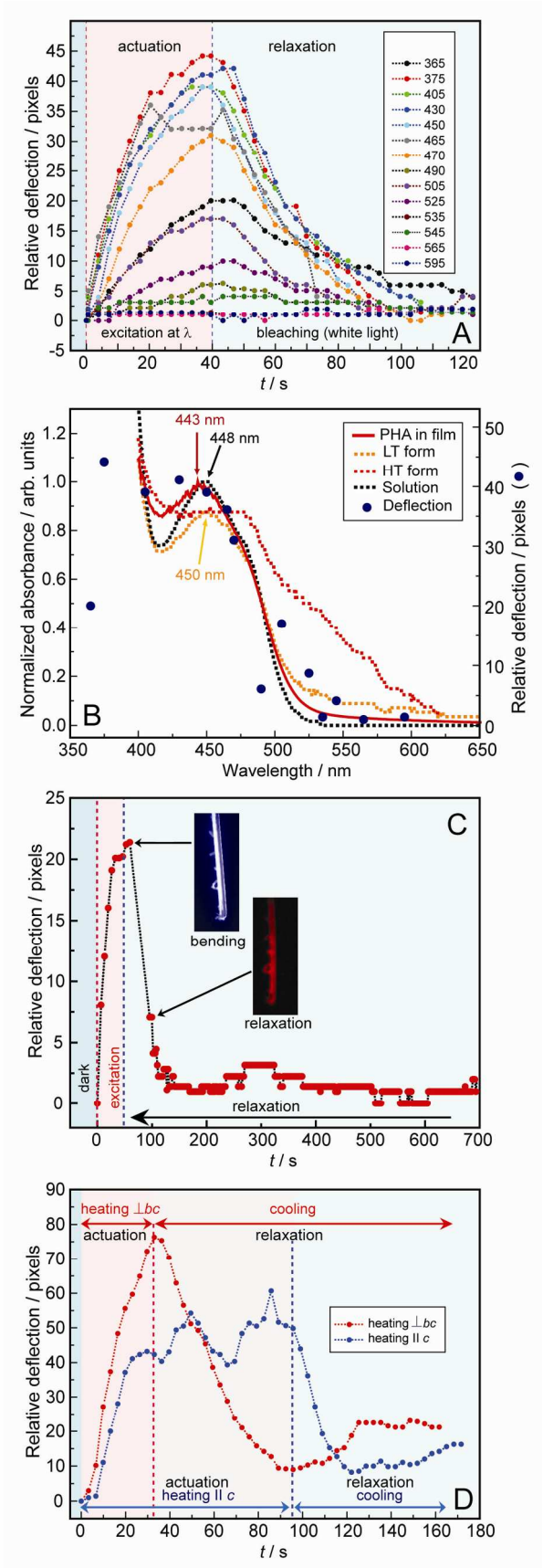

Fig. 3 Response and shape recovery of the PHA-doped sodium caseinate film to excitation by light and heat traced by the relative deflection of the film tip. (A) 40–second exposure to weak LED light induces nearly maximal deformation. The original shape is recovered by exposure to white light. (B) Absorption spectra of the two polymorphs, toluene solution and the PHA–doped film, co-plotted with the maximum deflection. The deflection depends on the excitation wavelength and reproduces the absorption spectra of the yellow form of PHA (low– temperature, LT), thus confirming the identity of the PHA as the yellow polymorph. (C) The shape of a photochemically bent film reverts in about one minute of being in the dark. After bending by 40-second exposure to UV light, the tip of the film was traced by recording, in 2–s intervals, 100μs stroboscopic flashes at 630 nm where it is optically transparent and remains unbleached. A secondary "echo effect" is observed around 300 s from the irradiation onset. The insets show images of the maximally bent film and a snapshot of the film after the dark period, showing that the shape of the film. (D) Thermally bending of the film induced by lateral (⊥***bc***, 30 s) or axial (||***c***; J) heating and recovery. The echo effect is also observed, evidencing that its origin is not photoexcitation but the mechanical deformation of the film.

3D). This observation provides proof to support the concept for potentially utilizing this and similar hybrid materials as heat-to-work converters. If kept within a temperature gradient between a heater and thermal sink, a miniature hybrid actuating element based on the hybrid thermosalient material is capable of performing mechanical work by oscillating between the heater and the sink. Another observation worth of note is the echo effect—a very small bending that occurs about 50–60 s after the heating has been terminated, where the film bends slightly to recover the former, bent shape (see the discussion below).

During the characterization of the hybrid material, we accidently discovered that the as−obtained films are also responsive to excitation by light (Figure 2A–E). When the free terminus of a hanging PHA−doped beam is exposed to weak UV light from a set of LEDs (λ_{max} = 405 nm) fixed around the film radially and perpendicular to its longest side, it bends visibly (Figure 2A–E). The bending was gradual and the maximal deflection of 5.6° was reached after 40 seconds irradiation (Figure 1E, F). The direction of bending was inherent to the anisotropy of the sample and did not depend on the direction of the excitation. The film retains the curved shape in the dark, but the initial straight shape can be recovered in less than 2 minutes if the film is exposed to weak white LED light. The bending can be repeated many times without notable fatigue. As seen in the SEM images in Figure S5 (SI), if a pristine film is exposed to strong UV light (order ~100 mW/cm^{-2}) many of the crystals jump out of their pockets or sublime. Films treated in such way show reduced mechanical response, in line with the fact that the crystals of PHA are the main driving elements behind the film actuation.

To provide additional evidence that the bending is indeed induced by photoexcitation and is not a heating artefact, we examined the dependence of the photomechanical effect on the wavelength. The excitation wavelength was varied between 365 nm and 595 nm with a set of replaceable LEDs fixed radially and equidistantly around the sample and controlled with an external controlling unit (the films were not photoresponsive to visible light with λ > 595 nm). During the 40-second exposure, the film deflected between 0.2 and 6°. The bending angle, at identical exposure time, depended strongly on the wavelength (see Fig. 4 and also Figure S4 and Movies S1–S14 in the SI). The strongest bending was observed with UV light (~375 nm, 6.0°) and blue light (~430 nm, 5.8°). As shown in Fig. 3B, the plot showing the dependence of the deflection (at t = 40 s) on the emission wavelength reproduces faithfully the absorption spectrum of the yellow (α) form of PHA and its toluene solution, where the molecules exist as discrete coordinated entities, and it is very

different from that of the high-temperature, red form (β). This result evidences that the coordination of PHA is preserved in the film, and that the light excited the electronic transitions. Moreover, the LEDs emit negligible heat, and therefore the light–induced bending is clearly a photoinduced effect and not a result of heating. Similar to the thermally induced bending, the photoinduced deformation was also accompanied by the echo effect. This observation supports the conclusion that the origin of this memory−like effect is not related to the photo– or thermal excitation; instead, it is a latent effect inherent to the material that appears in response to the mechanical deformation. The DFT-calculated transitions of PHA in form α show that the lowest two energy band originate from HOMO→LUMO, HOMO-1→LUMO, and HOMO-2→LUMO transitions which are essentially MLCT $d\rightarrow\pi^*$ transitions and $\pi\rightarrow\pi^*$ transitions of the ligand (the details of the calculations will be published elsewhere).

Being capable of dual response (to temperature and light), the new hybrid material provides the possibility of motion control by alternating thermo– and photoexcitation. To verify this, the same beam used to record the heat and photoinduced response was placed between sources of heat and weak UV light. As shown in Figures 2L–Q, when heated, the beam deflected toward the heat source. After cooling, it straightened back to its original shape. Excitation from the opposite side induced bending toward the light source that is to the opposite side. After termination of the photoexcitation, the beam returned to its original, straight shape. Alternating excitation by heat and light drives continuous oscillations, and the direction of the response (opposite or identical side) depends on the direction of the front face of the film. This result provides direct evidence that the hybrid material can be utilized as a multiresponsive smart medium for alternative conversion of heat and light into mechanical work.

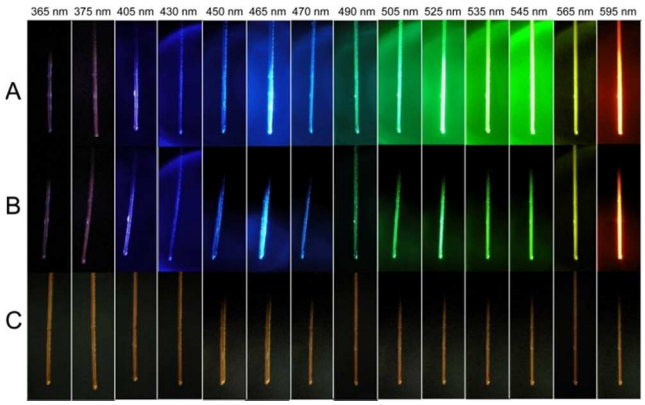

Fig. 4 Dependence of the mechanical response of a PHA–doped sodium caseinate film (Fig. 1) on the wavelength of the exci-tation light. Exposure to a set of LEDs of the film (A) induces various degrees of bending in about one minute (B). The original shape is restored by exposure to white light (C). The film responds only to light in the region 365–545 nm, and the deflection depends on the excitation wavelength.

Cytotoxicity tests

To confirm the potentials for utility of the hybrid materials towards application as artificial tissues in future, the cytotoxicity of doped and non-doped NaCas films was evaluated together with pure PHA against two cancer cell lines (Figure S6, SI), M8 (melanoma cancer cell line), and A549 (lung cancer cell line). Cells were treated with each compound for 48 h, followed by measuring the cell growth rates through a colorimetric assay (sulforhodamine-B assay) as described in the experimental section. The method that we utilized is known to accurately reflect the levels of total cellular macromolecules/cell growth/proliferation. The IC50 for each compound was calculated with reference to doxorubicin as a positive and DMSO as a negative control which represents the concentration that results in a 50% decrease in cell growth after 48 h incubation at 37 °C in the presence of compounds under study. For each compound, 50% growth inhibition was calculated from sigmoidal dose–response curves. As could be concluded from the cells survival Figures S6 (SI), all compounds were found to be non-cytotoxic against both M8 and A549 cell lines.[40] Since these compounds are not cytotoxic to cancer cell lines in which all proteomics are overexpressed compared to normal cells, we anticipate that they are safe for human uses. Further analysis and toxicity studies are under way in our laboratories to con-firm this claim.

Experimental

Preparation of the films

PHA was prepared according to a previously published procedure[39] and recrystallized by slow evaporation, at room temperature, from toluene or butyronitrile. PHA-doped films were prepared similar to published procedure.[41-42] For inclusion in the films, 0.05 g PHA was dissolved in 2 mL DMF with heating. Two types of films with different dopant–matrix ratios were prepared; the more diluted film exhibited better elastic properties and was used for optical and mechanical characterization. 0.5 g (or 0.25 g) of sodium caseinate (NaCas) were mixed with 9 mL (or 4 mL) water, and 10 (or 5) drops of glycerol were added. The mixture was stirred and heated in the water bath at ∼70 °C until dissolution, and the solution of PHA was added. At occasions when PHA precipitated, the heating was continued until dissolution, transferred to a polystyrene Petri dish, and dried in a desiccator at 23 °C over silica gel (RH ∼ 22%) during a couple of days, whereupon PHA crystallized within the gel.

Thermal analysis

Thermal properties (DSC) were analyzed with differential scanning calorimeter (DSC Q2000, TA) instrument, at a heating rate of 10 °C/min in the temperature range of 20–200 °C. Tzero alumina pans with an auto sampler were used for each DSC measurement. Similarly, thermogravimetric analyses were measured using (TGA SDT Q600, TA) at a heating rate of 10 °C/min using alumina pans. The temperature range for the TGA analysis was 20–700 °C. Dry N_2 gas was used as carrier gas for each measurement.

Spectroscopy

The UV–visible spectra were recorded at room temperature in absorption mode with a Shimadzu UV–3600 UV–Vis–NIR spectrometer. The spectrum of the PHA–doped NaCas was recorded directly by inserting the film in the beam path, followed by scaling. To record the spectra of the pure phases of the two polymorphs of PHA, which were prepared by recrystallization,

the crystals were thinly spread on self–adhesive tape using the clean tape to record the background. For recording of the solution-state spectra, PHA was dissolved in spectral–grade toluene and the concentration was adjusted to maximum absorbance of 0.26. The nuclear magnetic resonance (NMR) spectra of the non–doped samples were recorded on a Bruker Advance 400 MHz spectrometer with D_2O as solvent.

Scanning Electron Microscopy

Scanning electron microscopy (SEM) micrographs were taken with a QUANTA FEG 450 electron microscope with primary electron energy of 3–5 kV. The films were directly attached to adhesive carbon tapes. The micrographs were recorded at room temperature at pressure of 100 Pa. As revealed in Figure 1, the dopant is uniformly distributed over the polymeric matrixes as rod–like crystals.

Tensile testing

All specimens were tested at 25 °C. In the tensile tests, a sample with an oblong shape (4 × 0.5 cm) was placed in the grips of movable and stationary fixtures in a screw–driven device using KSU 05M tensile testing equipment (Universal Testing Ma-chine Co., Ltd), which pulls the sample until breaking, while recording the applied load versus elongation. The load cell and extensometer were calibrated prior to use. Load was applied at a crosshead speed 10 mm min^{-1}, and the load range was 0–500 N. The tests complied with rules specified by the international standard norms. For proper calculation, the average value and standard deviations were calculated out of a minimum of three specimens.

Photomechanical actuation

Strips of the PHA–doped NaCas typically measuring ~ 2 × 11 × 0.2 mm were cut out and affixed with glue to glass rods. The orientation and position of the hanging samples were con-trolled with an XYZ micromanipulator, and the movies were recorded with a digital camera (30 fps) coupled to a horizontal microscope. The photomechanical properties were studied by a setup consisting of six light emitting diodes (LEDs) which were attached to the sockets of a metal ring distributed radially at identical distance around the sample. The timing and synchronization of the LEDs was controlled with a custom-made external controlling unit connected to a PC. The excitation wavelength was tuned by replacing the LEDs with LEDs that emit between 365 nm and 595 nm (the films were not photoresponsive above 595 nm and thus longer wavelengths were not used for excitation).The recovery of the films in the dark was studied on a sample which was bent by a 60 s exposure to 405 nm (5 LEDs). To monitor the shape recovery, at 2 s intervals the bent sample was flashed 100 μs at 630 nm, where the film is optically transparent and remains unbleached. The tip of the film used was monitored over time. To study the thermomechanical response, the hanging films were heated either with a thermoelectric element from the lower side, or with an axially disposed electrically conducting wire heater mounted on an XYZ–micromanipulator.

Kinematics analysis

Kinematic analysis was carried out by using the computer program Hot Shot Link (Version 1.2) which allows the user to determine (x, y) coordinates of a point with respect to the origin (0, 0) on the program window. Inclination of the polymer film tip at different times were extracted as (x, y) by selecting a point on the polymer film tip (Figure S3). The first frame (inclination = 0, time = 0) corresponds to the first frame immediately after the UV light was turned on. The (x, y) coordinates were extracted at different times. The deflection of the film relative to the position in the first frame was calculated in pixels, by using $d = [(x_2–x_1)^2 + (y_2–y_1)^2]^{1/2}$, where the $x_{1,2}$ and $y_{1,2}$ are the x and y coordinates of two consecutive points.

Cell lines and culture conditions

Two human cancer cell lines were used in this study; A549 (lung cancer cell line) and melanoma (M8) and were maintained in Dulbecco's Modified Eagle's Medium (DMEM: Gibco, USA) supplemented with 10% fetal bovine serum (Gibco) and penicillin/streptomycin (Gibco). All incubations were done at 37 °C in a humidified atmosphere of 5% CO_2. Mycoplasma was tested at 3 month intervals.

Chemosensitivity assay and data analysis

Stock solutions of all compounds were prepared by dissolution in dimethyl sulphoxide (DMSO) and kept frozen at –80 °C. The appropriate concentrations used in the experiments were prepared by serial dilution in DMEM medium from the stock solution just before doing the experiment. The highest DMSO concentration did not exceed 2% in all the chemosensitivity experiments. Cytotoxicity of the compounds was determined using sulphorhodamine–B (SRB) method. Exponentially growing cells were seeded into 96–well microliter plates at a concentration of 5×103 cells/well. After 24 h, cells were incubated with either drug-free medium, medium–containing DMSO, or the compound (s) at different concentrations (0.1–100 μg/mL). At least, triplicate wells were prepared for each concentration. Following 48 h incubation at 37°Cin a humidified atmosphere of 5% CO2, cells were fixed for 1 hour at 4°C after adding 50 μL 50% trichloroacetic acid (TCA) to each well containing 200 μL. Plates were washed several times with tap water, air dried and stained with 0.4% SRB for 30 min and then washed several times with 1% acetic acid to remove unbound stain. Plates were air dried and the dye was solubilized with 10 mM Tris base (pH 10.5). The optical density was measured spectrophotometrically at 564 nm with an ELISA micro plate reader (Meter tech. S960, USA). Fractions of viable cells remaining for each concentration was calculated by dividing the reading at the respective concentration over the control untreated cells after subtracting the absorbance of cells incubated with DMSO alone (to ac-count for the DMSO effect). Survival curves were constructed by drawing the fraction of viable remaining cells against the concentrations used. The IC50 values were calculated using sigmoidal concentration–response curve fitting models (Graph Pad, Prism software). Statistical analysis, data fitting and graphics were performed by the Prism 3.1 computer program (GraphPad Software, USA). Data are given as mean ±SEM.

Conclusions

In conclusion, we have prepared a prototypic hybrid material

based on the thermosalient effect that can be actuated by temperature and light. Taken together, the results presented here show a conceptually new approach and strategy for the design of self–actuating smart materials. We have demonstrated that microcrystallites of thermosalient crystals, which when in pure form can leap when heated or cooled, can effectively actuate thin films of sodium caseinate as a biocompatible, natural protein matrix. The protein acts like an elastic and mechanically reinforcing medium which alleviates the propensity of thermosalient crystals for disintegration. The spectroscopic signature, kinematic performance and mechanical profile of the hybrid material are consistent with a mechanism where the thermosalient crystallites of the dopant act cooperatively to induce macroscopic mechanical deformation within the matrix. The hybrid material thus effectively mimics a muscle, with the crystals acting as a mechanically active backbone and the protein being the equivalent of the tissue. We proved that the coordination structure of the dopant is retained. Removal of the crystals of the actuating materials by exposure to very strong UV light leads to deterioration or loss of the actuating capability. In addition to heating, the new hybrid material also responds mechanically to excitation by very weak ultraviolet or blue light, therefore setting the platform for a new class of biocompatible actuators capable of dual mechanical actuation. The mechanism of the photoinduced excitation remains unclear; because the ligand is blocked for isomerization by the coordination, we suggest that the photoactuation occurs in response to structural changes in the coordination geometry induced by photoexcitation, or alternatively, as a result of *trans–cis* isomerization of small amount of free ligands in the crystal. Studies are now underway to clarify the mechanism. Notably, the hybrid material also displays improved tensile properties relative to the nondoped polymer and conveniently combines the fast energy transfer in single crystals and the elasticity of the natural polymer. As shown by the biocompatibility tests, the material is non–toxic, which stands as an important prerequisite towards biocompatibility. We believe that the potential application of this concept extends beyond the system described here, and by setting the basis for a new class of biocompatible actuating materials its relevance is more general.

Acknowledgements

We thank Dr. Boris-Marko Kukovec for the discussion on the synthetic procedures in the initial stages of the work on this subject, Dr. Reza Rowshan for his help with the SEM experiments, and Mr. Bailey Cuzzard for the fabrication of the molds.

Notes and references

[a] *New York University Abu Dhabi, PO Box 129188, Abu Dhabi, united Arab Emirates. E-mail: pance.naumov@nyu.edu*
[b] *College of Pharmacy, University of Sharjah, Po Box 27272, Sharjah, United Arab Emirates.*

† Electronic Supplementary Information (ESI) available: [SEM micrograph, mechanical bending movies, TGA, cytotoxicity tests]. See DOI: 10.1039/b000000x/

References

1 Y. Osada, H. Okuzaki, and H. Hori, *Nature,* 1992, **355**, 242.
2 R Pelrine, R. Kornbluh, Q. Pei and J. Joseph, *Science,* 2000, **287**, 836.
3 W. Lu, A. G. Fadeev, B. Qi, E. Smela, B. R. Mattes, J. Ding, G. M. Spinks, J. Mazurkiewicz, D. Zhou, G. G. Wallace, D. R. MacFarlane, S. A. Forsyth and M. Forsyth, *Science*, 2002, **297**, 983.
4 R. H. Baughman, C. Cui, A. A. Zakhidov, Z. Iqbal, J. N. Barisci, G. M. Spinks, G. G. Wallace, A. Mazzoldi, D. De Rossi, A. G. Rinzler, O. Jaschinski, S. Roth and M. Kertesz, *Science,* 1999, **284**,1340.
5 Kim, P.; Lieber, C. M. *Science,* 1999, **286**, 2148..
6 Y. Osada and D. E. E. Derossi, Polymer sensors and actuators, Springer, Berlin, 2000.
7 E. Smela, *Adv. Mater*., 2003, **15**, 481.
8 G. M. Spinks, G. G. Wallace, L. S. Fifield, L. R. Dalton, A. Mazzoldi, D. De Rossi, I. I. Khayrullin and R. H. Baughman, *Adv. Mater*., 2002, **14**, 1728.
9 M.-H. Li, P. Keller, B. Li, X. Wang, M. Brunet, *Adv. Mater*., 2003, **15**, 569.
10 H. Finkelmann, E. Nishikawa, G. G. Pereira and M. Warner, *Phys. Rev. Lett*., 2001, 87, 015501.
11 P. M. Hogan, A. R. Tajbakhsh and E. M. Terentjev, *Phys. Rev*., 2002, **E65**, 041720.
12 A. Natansohn, P. Rochon, *Chem. Rev*., 2002, **102**, 4139.
13 G. Smets and F. De Blauwe, *Pure Appl. Chem*., 1974, **39**, 225.
14 C. D. Eisenbach, *Polymer,* 1980, **21**, 1175.
15 L. Matějka, M. Ilavský, K. Dušek and O. Wichterle, *Polymer*, 1981, **22**, 1511.
16 Y. Yu, M. Nakano and T. Ikeda, *Nature,* 2003, **425**, 145.
17 T. Ikeda, M. Nakano, Y. Yu and O. Tsutsumi, A. Kanazawa, *Adv. Mater*., 2003, **15**, 201.
18 M. Kondo, Y. Yu and T. Ikeda, *Angew. Chem., Int. Ed*., 2006, **45**, 1378.
19 Y. Yu, T. Maeda, J. Mamiya, T. Ikeda, *Angew. Chem., Int. Ed*., 2007, **46**, 881.
20 Y. Yu, M. Nakano, T. Ikeda, *Pure Appl. Chem.,* 2004, **76**, 1435.
21 M.-H. Li, P. Keller, B. Li, X. Wang and Brunet, M. *Adv. Mater*., 2003, **15**, 569.
22 P. M. Hogan, A. R. Tajbakhsh, E. M. Terentjev, *Phys. Rev*. 2002, **E 65**, 041720-1.
23 M. Yamada, M. Kondo, J. Mamiya, Y. Yu, M. Kinoshita, C. J. Barrett and T. Ikeda, *Angew. Chem., Int. Ed*., 2008, **47**, 4986.
24 G. A. Shandryuk, S. A. Kuptsov, A. M. Shatalova, N. A. Plate, R. V. Talroze, *Macromolecules*, 2003, **36**, 3417.
25 G. N. Mol, K. D. Harris, C. W. M. Bastiaansen and D. J. Broer, Adv. Funct. Mater., 2005, 15, 1155.
26 J. Naciri, A. Srinivasan, H. Jeon, N. Nikolov, P. Keller and B. R. Ratna, *Macromolecules*, 2003, **36**, 8499.
27 M. Warner and E. M. Terentjev, Liquid Crystal Elastomers, Oxford University Press, Oxford, 2003.
28 D. L. Thomsen III, P. Keller, J. Naciri, R. Pink, H. Jeon, D. Shenoy and B. R. Ratna, *Macromolecules*, 2001, **34**, 5868.
29 S. Kobatake, S. Takami, H. Muto, T. Ishikawa and M. Irie, *Nature*, 2007, **446**, 778.
30 F. Terao, M. Morimoto and M. Irie, Angew. Chem., Int. Ed., 2012, 51, 901.
31 L. Kuroki, S. Takami, K. Yoza, M. Morimoto and M. Irie, *Photochem. Photobiol. Sci*., 2010, **9**, 221.
32 M. Morimoto and M. Irie, *J. Am. Chem. Soc*., 2010, **132**, 14172.
33 K. Uchino and M. Aizawa, *Jpn. J. Appl. Phys*., 1985, **24**, 139.
34 B. Feringa, R. A. van Delden, N. Koumura and E. M. Geertsema, *Chem. Rev*., 2000, **100**, 1789.
35 A. Yildiz, J. N. Forkey, S. A. McKinney, T. Ha, Y. E. Goldman and P. R. Selvin, *Science*, 2003, **300**, 2061.
36 T.–A. V. Khuong, J. E. Nuñez, C. E. Godinez and M. A. Garcia-Garibay, *Acc. Chem. Res*., 2006, **39**, 413.
37 J. D. Dunitz, J. Bernstein, Disappearing polymorphs, *Acc. Chem. Res*., 1995, **28**, 193.
38 J. Bernstein, Polymorphism in Molecular Crystals; Oxford University Press: Oxford, 2002; p. 223.
39 M. C. Etter and A. R. Siedle, *J. Am. Chem. Soc.,* 1983, **105**, 641.
40 R. A. El–Awady, E. M. Saleh, M. Ezz and A. M. El–sayed, *Toxicol.*

Appl. Pharmacol., 2011, **255**, 271.
41 M. Behl and Lendlein, A., *Soft Matter*, 2007, **3**, 58.
42 P. Frohberga, M. Pietzschb and J. Ulrich, *Chem. Eng. Res. Des*., 2010, **88**, 1148.

Table of Contents Entry

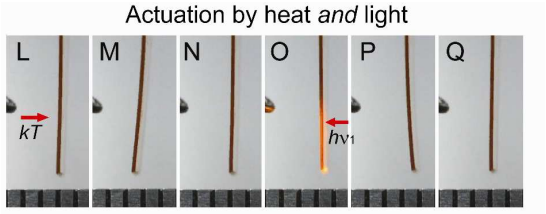

Crystals of a thermosalient (jumping) solid were employed as mechanically active "backbone" to actuate a "tissue" from natural protein matrix by both light and heat in a way similar to actuation in muscles.